JOURNAL OF SOLID STATE CHEMISTRY 117, 294–299 (1995)

Metastable Nitride Synthesis by Pulsed Laser Deposition: A New Phase in the NbN_x System

Randolph E. Treece,[1] James S. Horwitz, Syed B. Qadri, Earl F. Skelton, Edward P. Donovan and Douglas B. Chrisey

Naval Research Laboratory, Washington, DC 20375-5345

Received August 28, 1994; in revised form November 9, 1994; accepted November 9, 1994

Pulsed laser deposition (PLD) has been used to grow a series of NbN_x ($0 \leq x \leq 1.2$) thin-film materials, including a new superconducting phase. The structural and electrical properties of the NbN_x films were characterized. Structural analysis of the new NbN phase indicates that it is stabilized by heteroepitaxial growth on (100) MgO and is shown to be a primitive cubic distortion from the typical B1, or rock-salt structure. In addition, the NbN phase has a higher superconducting critical temperature and a larger lattice parameter when compared with films of B1-NbN. Growth of this new phase demonstrates that the nonequilibrium synthesis properties of PLD can be used to deposit new, metastable materials. © 1995 Academic Press, Inc.

INTRODUCTION

Traditional synthetic approaches to solid-state chemistry utilize high temperatures for long durations to overcome diffusion limitations. These high-temperature methods usually result in thermodynamically stable phases. A considerable amount of effort has been applied to develop synthetic methods which allow for greater control over product phase (including metastable structures) (1). Precipitation and low-temperature thermolysis of single-source precursors (2), the sol–gel process (3), and solid-state metathesis (SSM) reactions (4) all have been developed to address the limitations of traditional solid-state chemistry techniques.

An alternative approach to bulk synthesis is to deposit new materials in thin-film form. While many thin-film deposition techniques are limited in their control over the product phase, we are developing pulsed laser deposition (PLD) as a new synthetic technique to enable the preparation of metastable materials. In PLD, short (30 nsec), high-energy laser pulses are focused onto a solid target material. Rapid heating, vaporization, and ionization of the material results in a dense plasma above the target. The vapor is collected on a nearby substrate. While PLD has been used to grow a variety of compounds, it has been used most extensively for the deposition of complex oxides, such as high-temperature superconductors and ferroelectric compounds (5). Among the advantages of PLD as a synthetic technique for the formation of metastable compounds are the ability to operate in large background pressures ($\leq$ 1 Torr) of reactive gases, the high energies of ablated species ($\leq$ 100 eV), and the very high instantaneous growth rates ($\leq 10^5$ Å/sec) (6). PLD has been used to deposit films of metastable compounds, such as the infinite layer oxides $Ca_{1-x}Sr_xCuO_2$ (7), cubic boron nitride (8), and carbon nitride (CN_x) (9, 10).

This paper will describe how our group has applied PLD to the synthesis of nitride materials. We have investigated the growth of the nitrides of niobium (NbN_x) by PLD (11–14). The early transition metals usually can form several different, and sometimes metastable, nitride phases as the nitrogen to metal ratios are changed (15). The nonstoichiometric nature of the transition metal nitrides complicates the phase assignment of NbN_x materials. The nonstoichiometries can be present as vacancies or defects on either the nonmetal or metal sublattices, or both, within a given phase (15). The rock-salt (B1) phase of niobium nitride is a refractory material with a bulk superconducting transition temperature (T_c) of ~16 K (15). Thin films of NbN also are being studied for applications in electronics. The low chemical reactivity, mechanical durability, high T_c ($T_c \gg 4.2$ K), and ease with which Josephson junctions can be reproducibly manufactured make NbN a good candidate for use in low-temperature digital electronics (16).

EXPERIMENTAL

The nitride films were grown in a high-vacuum chamber equipped with a cryopump and a turbomolecular pump, as shown in Fig. 1. A pulsed KrF excimer laser beam (248 nm, 30 nsec FWHM) operating at 10 Hz was focused with a 50-cm focal length lens at 45° onto a dithering and rotating (30 rpm) Nb target. The ambient gas (N_2 with 10%

[1] Author to whom correspondence should be addressed.

0022-4596/95 $12.00

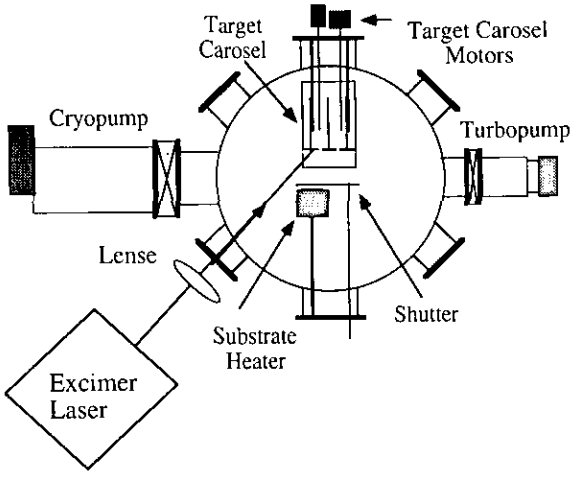

FIG. 1. Pulsed laser deposition system.

H_2) input pressure was regulated to a dynamic equilibrium (~10 sccm) by a solenoid-activated leak valve controlled by a capacitance manometer with the chamber under gated or throttled pumping. The substrates were washed with ethanol, attached to the substrate heater with silver paste, and maintained ~6 cm from the target. The laser fluence was 6 J/cm^2. The film compositions and thicknesses were determined by Rutherford backscattering spectroscopy (RBS) with 6 MeV He^{2+}. X-Ray diffraction patterns were collected using a rotating anode source and a conventional θ–2θ geometry and indexed using a least-squares fit of the data. Γ (FWHM) for a particular reflection was measured by fixing 2θ at the peak maximum and scanning through θ. Oscillation photographs also were recorded of several films to confirm the assigned structure. Temperature-dependent resistance ($R(T)$) measurements were performed by a standard ac four-point probe measurement. J_c (4.2 K) was measured inductively as previously described (17).

RESULTS AND DISCUSSION

Gas Pressure and NbN_x Composition

Thin films of NbN_x were prepared by PLD of Nb under N_2/(10 %) H_2 ambient. In order to determine the effect of gas pressure on NbN_x composition a series of films was grown on (100) MgO substrates held at a deposition temperature (T_{sub}) of 600 °C at a variety of pressures. In general, the nitrogen content in the NbN_x films was found to increase with gas pressure.

The XRD pattern of the film deposited at a pressure of 10^{-7} Torr (Fig. 2, bottom) is consistent with textured niobium (18) and was indexed with a cubic lattice constant of a = 3.335(1) Å. Further evidence for strong texturing was seen by a θ scan, where Γ (200) = 1.7 °θ. The fitted RBS spectra indicated that no nitrogen was present in the film, as expected for films deposited under vacuum. The Nb film displayed metallic behavior as it was cooled to its superconducting transition at T_c (R = 0) of 9.2 K. This value is indicative of a high-quality niobium film (19).

At gas pressures between 1 and 20 mTorr, the deposited films yielded XRD patterns which could be indexed as hexagonal Nb_2N with lattice constants consistent with reported values (20). A representative XRD pattern is shown in Fig. 2 (first pattern up from the bottom). The films displayed strong (100) texturing. The lattice parameters for the films grown at 1, 10, and 20 mTorr were calculated to be a = 3.10(1) Å and c= 4.82(1) Å, a = 3.16 Å and c = 4.90(1) Å, and a = 3.10(1) Å and $c \leq$ 5.01(1) Å, respectively. Fits of RBS spectra revealed that the amount of nitrogen incorporated into the Nb_2N structure increased with reactive gas pressure, as shown in Fig. 3. Figure 3 shows the transition temperature and nitrogen content plotted as a function of deposition pressure. The observation of Nb_2N phases with a range of compositions is consistent with phase diagrams of the Nb–N system (15). The resistivity slightly decreased with temperature to an abrupt change below 5 K where there was an onset to a superconductive transition which did not go to R = 0 before 4.2 K. Previous investigations have noted metallic character and a lack of superconductivity above 4.2 K for Nb_2N (21).

At 60 mTorr, the XRD patterns of the deposited films (Fig. 2, second pattern up from the bottom) could be readily identified as cubic with lattice parameters for all of the films exceeding 4.4 Å. The films were highly textured in (100) orientation with the substrate. The XRD pattern contained odd (h00) reflections indicative of a primitive cubic distortion from the well-known rock-salt

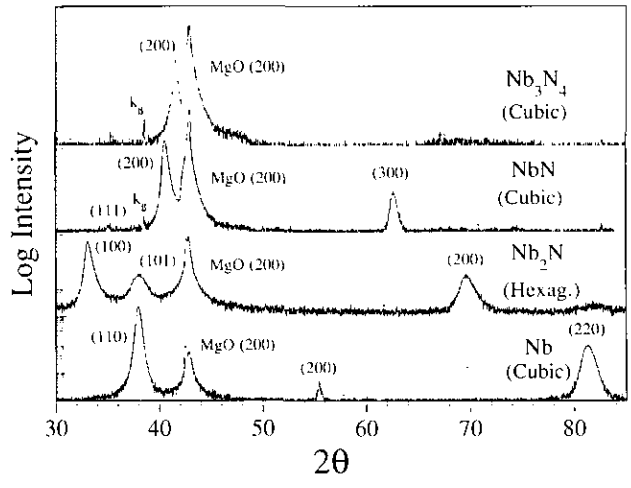

FIG. 2. Representative XRD patterns of NbN_x phases grown on (100) MgO by PLD. Miller indices and structure are indicated.

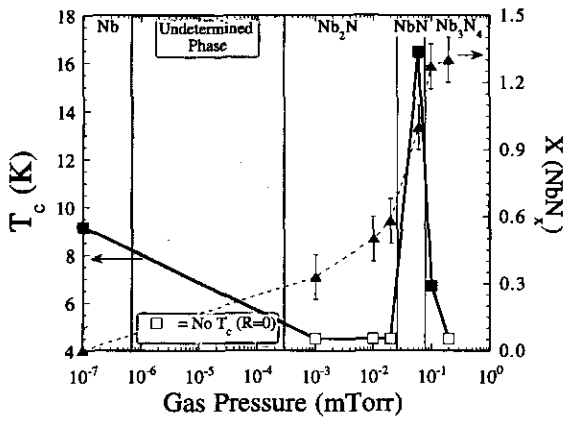

FIG. 3. Transition temperature and x value for NbN_x plotted as function of N_2/H_2 (10%) gas pressure. The NbN_x structural phases are indicated for specific pressure ranges. The "undetermined phase" region of pressures was not investigated.

NbN unit cell (22). (This new structure is discussed further in the next section.) A θ scan of the film also indicated strong texturing with Γ (200) = 1.2° θ. Analysis of the RBS spectra of films grown at 60 mTorr consistently indicated compositions of $NbN_{1.0}$. NbN displayed metallic behavior down to its T_c ($R = 0$) of 16.4 K. This is among the highest T_c's reported for a NbN film free of carbon impurities (known to raise T_c in NbN) (21, 23). Optimization of NbN films for superconducting applications is described elsewhere (12).

All of the films grown at pressures > 60 mTorr displayed cubic lattice constants ≤ 4.36 Å and nitrogen compositions ≈$NbN_{1.3}$. The unit cells of the highly textured films were determined to be cubic, based on the presence of (200) and (400), as seen in the NbN films . The film grown at 200 mTorr and had a = 4.343(1) Å and Γ (FWHM) = 0.8°θ, with a composition, given by RBS, of $NbN_{1.3}$. For the nitrogen-rich films ($x > 1$), resistance increased with decreasing temperature and displayed room-temperature resistivities several times higher than the other phases. Higher resistivities are consistent with properties previously reported for Nb_3N_4 (24). A decrease in the lattice constant of NbN_x with $x > 1$ is expected, since, for cubic materials with $x \approx 1$, the a's have been shown to increase with nitrogen content to a maximum when $x = 1$, and then decrease with increasing nitrogen incorporation. Bulk cubic NbN_x samples can maintain their structure over a broad range of x values ($0.86 \leq x \leq 1.1$) by incorporating N defects when $x < 1$ and Nb vacancies when $x > 1$ (15).

Substrate Temperature and Growth of the Metastable NbN Phase

XRD patterns of the films deposited at a pressure of 60 mTorr and substrate temperature of 600°C indicated that a new phase of NbN had been synthesized. The presence of a (300) peak in the XRD pattern suggested that a primitive cubic distortion of the B1 phase had occurred. The conditions under which the new phase could be deposited were investigated by varying the deposition temperature while holding the pressure at 60 mTorr. Based on their structural characteristics as revealed through the XRD patterns, the NbN films deposited at 60 mTorr and at a series of temperatures could be separated into two categories: those representative of the expected FCC lattice (22) and those of the primitive cubic (PC) lattice. Due to strong (h00) texturing, only the (200) and (400) reflections were observed in the FCC NbN films grown at substrate temperatures ≥150°C. Both groups of films are represented by the XRD patterns shown in Fig. 4a. All the (h00) peaks within the range of measurement were seen for both films, including the (300) line in the PC-NbN film (Fig. 4a, top pattern) forbidden by the $Fm3m$ symmetry of the B1 structure (Fig. 4a, bottom pattern).

The observation of the PC lattice was confirmed in

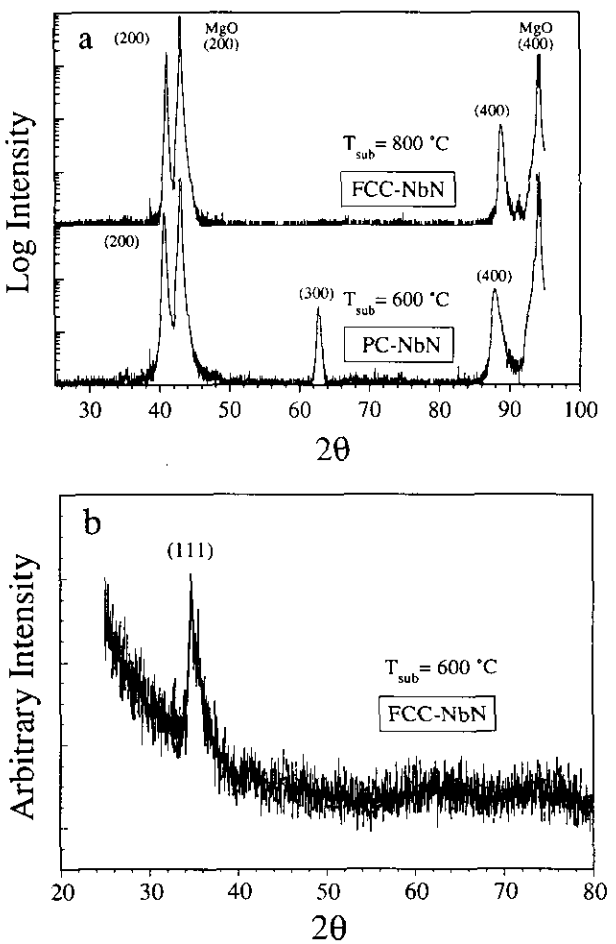

FIG. 4. XRD patterns of NbN films grown on (a) MgO substrates at 800°C and 600°C and on (b) amorphous fused silica at 600°C.

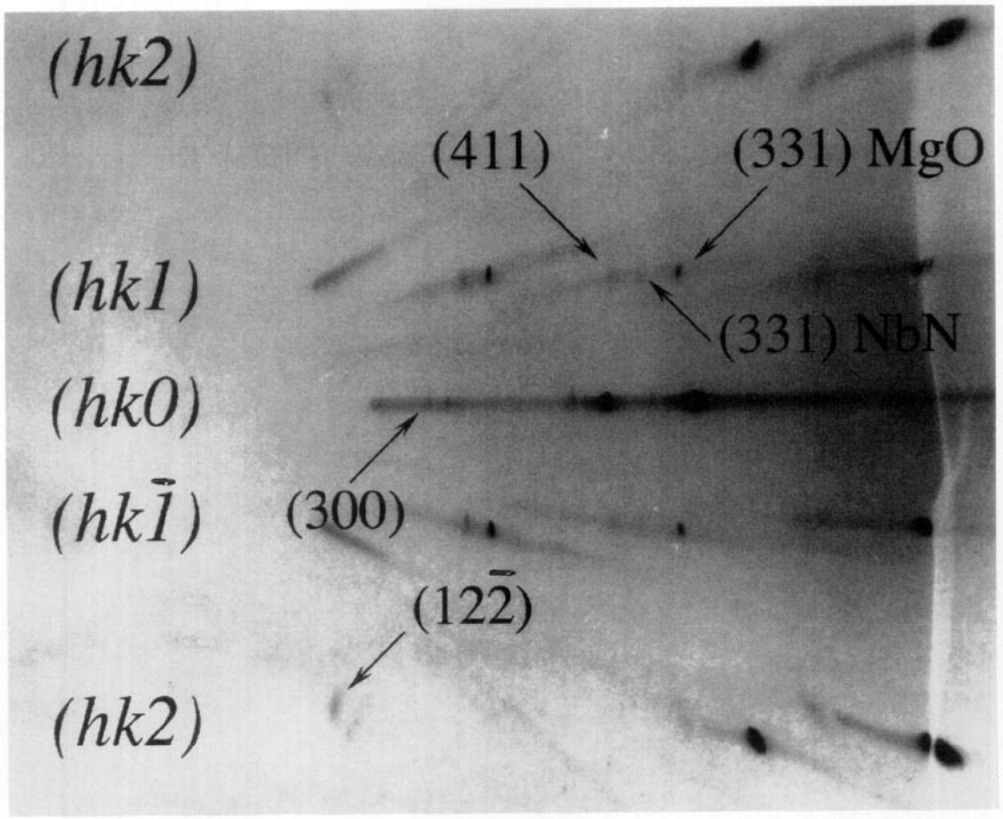

FIG. 5. Oscillation photograph of PC–NbN film on (100) MgO substrate. The diffraction planes and selected reflections are indicated. Note the (300), (411), and (12$\bar{2}$) diffraction spots of the NbN film characteristic of the primitive cubic phase.

an oscillation photograph. Figure 5 shows an oscillation photograph taken of a film whose XRD pattern indicated the new phase. Two sets of diffraction spots are present, one set from the single crystal MgO substrate and the other set from the deposited NbN film. The presence of spots for the NbN, instead of arcs or rings, indicates that it adopts heteroepitaxial orientation in the *ab* plane, as well as in the *c* direction. Each substrate spot also is associated with a film diffraction spot. The difference between the FCC lattice of the substrate and the PC lattice of the film is evidenced by the additional spots corresponding to the (300) reflection in the zero layer, the (411) reflection in the first layer, and the (12$\bar{2}$) reflection in the second layer, as indicated in the photograph. The (331) reflections for both the MgO substrate and NbN film also are indicated for reference. The lattice parameter of the PC-NbN film was found to be 4.442(2) Å from the oscillation photograph by plotting $(h^2 + k^2 + l^2)^{1/2}$ versus $1/d$ (Å). We further confirmed the PC lattice by using the orientation matrix to locate and measure the (411) reflection on the diffractometer (14).

The PC-NbN phase only could be stabilized over a narrow range of substrate deposition temperatures. The cubic lattice parameters of the deposited films were sensitive to substrate temperature and correlated with the NbN structural phase, as shown in Fig. 6. The film grown at room temperature (open triangle) was polycrystalline with a B1 structure and $a = 4.378(5)$ Å. The films grown at 150, 700, 800, and 900°C (closed squares) were highly (*h*00) oriented in the B1 phase with 4.408 Å $\leq a \leq$ 4.420 Å. When the substrate temperature was between 400 and 650°C (open squares), the deposited films adopted the PC lattice and displayed 4.438 Å $\leq a \leq$ 4.442 Å. This is consistent with what was observed with the oscillation photograph.

Film composition, as determined by RBS spectra, indicated that the films grown at temperatures of 150°C and above had the same compositions, within experimental error, with ratios of nitrogen to niobium of $1.0 \leq N/Nb \leq 1.1$. The film grown at room temperature had considerably more nitrogen present with N/Nb = 1.4. The deposited films were found by RBS to be free of oxygen and carbon contamination (25).

The PC-NbN films displayed high T_c's, sharp superconducting transitions, metallic resistivity dependence above T_c, and large critical currents. The PC-NbN films showed T_c ($R = 0$) $\approx$ 16.4 K values which exceeded the FCC-NbN films by greater than 0.5 K. In addition, the transition

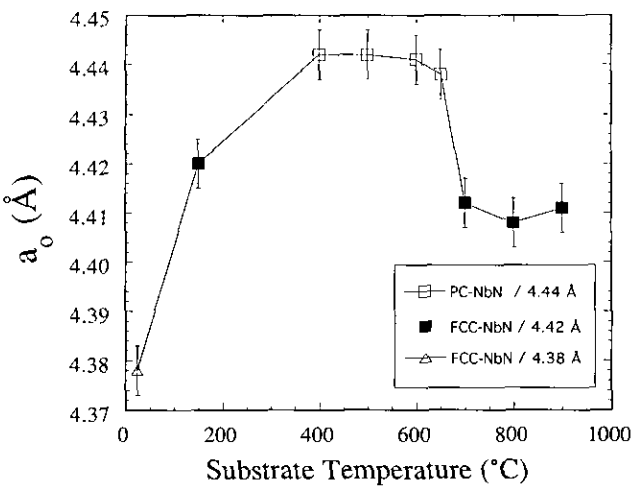

FIG. 6. Lattice parameters of NbN films are plotted as a function of substrate deposition temperature. The phase of the NbN and approximate lattice parameters are indicated in the legend.

widths were sharper for the PC phase (~0.2 K) than for the FCC material (1–3 K). The PC phase also displayed a metallic dependence of resistivity above T_c while the FCC phase showed an activated temperature dependence. The room-temperature resistivity was the same for both phases (~50 $\mu\Omega$-cm). The critical current (J_c) measured by inductive methods for a PC-NbN film was 7.1 MA/cm^2 (12).

Substrate Orientation and Stabilization of the New NbN Phase

The effect of the substrate on growth of the new phase was examined. The new phase grows heteroepitaxially in a (100) orientation on the (100) face of MgO, where the lattice mismatch between the PC-NbN (a = 4.44 Å) and the MgO substrate (a = 4.21 Å) is ~5%. To test whether the oriented substrate was required to stabilize PC–NbN, growth of the new phase on an amorphous substrate was attempted. When NbN films were deposited simultaneously on (100) MgO and amorphous SiO_2 at 600°C, the metastable phase only would grow on the MgO substrate. The film deposited on the fused silica was polycrystalline B1-NbN (as shown in Fig. 4b). The XRD pattern of the polycrystalline film can be compared to the that of a PC-NbN film grown on an MgO substrate (shown in Fig. 4a). The T_c (11.8 K), room-temperature resistivity (120 $\mu\Omega$-cm) and J_c (1.8 MA/cm^2) of the polycrystalline FCC–NbN film were depressed significantly below those of the PC-NbN material grown simultaneously on (100) MgO (T_c = 16.1 K, ρ = 60 $\mu\Omega$-cm, and J_c = 7.1 MA/cm^2).

Discussion of the New NbN Phase

This study has revealed trends in several physical characteristics which prove the existence of a new phase of NbN. These trends are a result of the rich Nb–N phase diagram and reflect the ability of PLD to synthesize new materials. Films deposited between 400 and 650°C and at 60 mTorr are single-phase NbN adopting the new structure. This new phase is manifested by a change in structure and transport properties from films deposited at substrate temperatures below 400°C and above 650°C, and could not be stabilized on an amorphous substrate.

The new NbN phase adopts a primitive cubic lattice and has a lattice parameter considerably larger than that of B1-NbN. The B1 phase of NbN has been shown to be a nonstoichiometric compound with substantial defects on the sublattices of each atom, up to 25 %. The a of bulk NbN has been shown to increase with N/Nb in nitrogen-deficient material (N/Nb < 1) to a maximum when N/Nb = 1. When N/Nb exceeds unity, the material becomes niobium deficient and the lattice parameter decreases as N/Nb increases. "Stoichiometric" NbN (i.e., N/Nb = 1), with a lattice parameter of 4.39 Å, is really $Nb_{0.97}N_{0.97}$, as determined by density measurements (15). The change in the unit cell and the increase in a seen in the new phase, is possibly due to increasing the occupancy of both N and Nb on their respective lattice sites. However, since RBS only yields information on the N/Nb ratio, it alone cannot resolve site occupancy. Modeling the XRD scans with various possible lattice defects, deficiencies, and interstitials based on modifications of the rock-salt structure also was inconclusive. Currently, there is insufficient data to effectively model the new NbN phase, but alternative structural analyses are being explored.

CONCLUSIONS

A new phase of superconducting NbN has been synthesized by the pulsed laser ablation of Nb foil in a reactive gas atmosphere and deposition on an oriented substrate. The new phase is stabilized by heteroepitaxial growth on (100) MgO substrates in a range of substrate deposition temperatures from 400 to 650°C. The structure of the new phase is a primitive cubic (PC) distortion of the well-known B1 form of NbN. Substrate deposition temperatures above and below that range resulted in oriented NbN in the B1 phase. The PC-NbN displays improved electronic transport properties and a larger lattice parameter relative to B1-NbN. Growth of the new phase may be due to unique aspects of PLD, such as the high energies of the ablated species (≤100 eV) and the very large instantaneous growth rates (≤10^5 Å/sec) associated with this deposition technique.

ACKNOWLEDGMENTS

The authors gratefully acknowledge Dr. M. S. Osofsky for many helpful discussions and the Office of Naval Research and the National

Research Council/Naval Research Laboratory Cooperative Postdoctoral Research Associate program (RET) for financial support.

REFERENCES

1. (a) A. Stein, S. W. Keller, and T. A. Mallouk, *Science* **259**, 1558 (1993). (b) R. Roy, *Solid State Ionics* **32**, 3 (1989).
2. A. Wold, *J. Chem. Educ.* **57**, 531 (1980).
3. (a) C. J. Brinker and G. W. Scherer, "Sol–Gel Science." Academic Press, New York, 1990; (b) E. Matijevic, *Chem. Mater.* **5**, 412 (1993); (c) J. Livage, M. Henry, and C. Sanchez, *Prog. Solid State Chem.* **18**, 259 (1988).
4. (a) J. B. Wiley and R. B. Kaner, *Science* **255**, 1093 (1992); (b) R. E. Treece, G. S. Macala, and R. B. Kaner, *Chem. Mater.* **4**, 9 (1992); (c) R. E. Treece, E. G. Gillan, R. M. Jacubinas, J. B. Wiley, and R. B. Kaner, *Mater. Res. Soc. Symp. Proc.* **271**,, 169 (1992); (d) R. E. Treece, G. S. Macala, L. Rao, D. Franke, H. Eckert, and R. B. Kaner, *Inorg. Chem.* **32**, 2745 (1993).
5. Growth of electronic ceramics by PLD is reviewed in J. S. Horwitz, D. B. Chrisey, K. S. Grabowski, and R. E. Leuchtner, *Surf. Coatings Technol.* **51**, 290 (1992).
6. D. B. Chrisey and G. K. Hubler (Eds.), "Pulsed Laser Deposition of Thin Films." Wiley, New York, 1994.
7. (a) C. Niu and C. M. Lieber, *J. Am. Chem. Soc.* **114**, 3570 (1992); (b) D. P. Norton, B. C. Chakoumakos, J. D. Budai, and D. H. Lowndes, *Appl. Phys. Lett.* **62**, 1679 (1993).
8. (a) A. K. Ballal, L. Salamanca-Riba, G. L. Doll, C. A. Yaylor II, and R. Clarke, *Mater. Res. Soc. Symp. Proc.* **285**, 513 (1993); (b) A. K. Ballal, L. Salamanca-Riba, C. A. Yaylor II, and G. L. Doll, *Thin Solid Films* **224**, 46 (1993); (c) F. Qian, V. Nagabushnam, and R. K. Singh, *Appl. Phys. Lett.* **63**, 317 (1993).
9. (a) F. Xiong and R.P.H. Chang, *Mater. Res. Soc. Symp. Proc.* **285**, 587 (1993); (b) C. Niu, Y.Z. Lu, and C.M. Lieber, *Science* **261**, 334 (1993).
10. R. E. Treece, J. S. Horwitz, and D. B. Chrisey, *Mater. Res. Soc. Symp. Proc.* **327**, 245 (1994).
11. R. E. Treece, J. S. Horwitz, and D. B. Chrisey, *Chem. Mater.* **6**, 2205 (1994).
12. R. E. Treece, J. S. Horwitz, J. H. Claassen, and D. B. Chrisey, *Appl. Phys. Lett.* **65**, 2860 (1994).
13. R. E. Treece, J. S. Horwitz, and D. B. Chrisey, *Mater. Res. Soc. Symp. Proc.* **343**, 747 (1994).
14. R. E. Treece, M. Osofsky, E. Skelton, S. Qadri, J. S. Horwitz, and D. B. Chrisey, *Phys. Rev. B.* **51**, *9356 (1995).*
15. L. E. Toth *in* "Transition Metal Carbides and Nitrides" (J. L. Margrave, Ed.), Refractory Materials, Vol. 7. Academic Press, New York, 1971.
16. H. Weinstock and M. Nisenoff, (Eds.), "Superconducting Electronics." Springer-Verlag, New York, 1992.
17. J. H. Claassen, M. E. Reeves, and R. J. Soulen, *Rev. Sci. Instrum.* **62**, 996 (1991).
18. Joint Committee on Powder Diffraction Standards, "Powder Diffraction File," 35-789 (Nb). International Center for Diffraction Data, Swarthmore, PA, 1986.
19. (a) J. H. Claassen, S. A. Wolf, S. B. Qadri, T. L. Francavilla, and L. D. Jones *J. Cryst. Growth* **81**, 557 (1987); (b) Y. Igarashi and M. Kanayama *J. Appl. Phys.* **57**, 849 (1985).
20. Joint Committee on Powder Diffraction Standards, "Powder Diffraction File," File 39-1398 (Nb_2N). International Center for Diffraction Data, Swarthmore, PA, 1986.
21. (a) S. A. Wolf, D. U. Gubser, T. L. Francavilla, and E. F. Skelton, *J. Vac. Sci. Technol.* **18**, 253 (1981); (b) E. J. Cukauskas, W. L. Carter, and S. B. Qadri, *J. Appl. Phys.* **57**, 2538 (1985); (c) A. Shoji, S. Kiryu, and S. Kohiro, *Appl. Phys. Lett.* **60**, 1624 (1992).
22. Joint Committee on Powder Diffraction Standards, "Powder Diffraction File" File 38-1155 (NbN). International Center for Diffraction Data, Swarthmore, PA, 1986.
23. A. Shoji, S. Kiryu, and S. Kohiro, *Appl. Phys. Lett.* **60**, 1624 (1992).
24. R. Fix, R. G. Gordon, and D. M. Hoffman, *Chem. Mater.* **5**, 614 (1993).
25. In these experiments, the RBS limit of detection for oxygen and carbon is about 5%.